*J*inst

Relativistic charged particle ejection from optical lattice

E.N. Frolov,[a,b,1] **A.V. Dik**[b,c] **and S.B. Dabagov**[b,c,d]

[a] *NR Tomsk Polytechnic University, Tomsk, Russia*
[b] *RAS P.N. Lebedev Physical Institute, Moscow, Russia*
[c] *NRNU MEPhI, Moscow, Russia*
[d] *INFN Laboratori Nazionali di Frascati, Frascati, Italy*

E-mail: frol.onn@gmail.com

ABSTRACT: We have analyzed relativistic (∼ MeV) electron ejection from potential channels of standing laser wave taking into account both rapid and averaged oscillations within the region of declining field of standing wave. We show that only a few last rapid oscillations can define transverse speed and, therefore, angle at which a particle leaves standing wave. This conclusion might drastically simplify numerical simulations of charged particles channeling and accompanying radiation in crossed lasers field. Moreover, it might provide a valuable information for estimation of charged particle beams parameters after their interaction with finite standing wave.

KEYWORDS: Accelerator modelling and simulations (multi-particle dynamics; single-particle dynamics); Beam dynamics; Beam Optics

---

[1]Corresponding author.

2018 JINST 13 C03042

Contents

1 Introduction

Charged particle dynamics in field of electromagnetic waves superposition is considered since first being addressed by P.L. Kapitza and P.A.M. Dirac [1]. Depending on interaction time, particle energy and field intensity diffraction and channeling regimes for charged particle are possible (see figure 5 at [2]). The latter regime allowing classical treatment is considered below. According to the Kapitza method the motion of charged particles in high-frequency gradient field could be treated as a superposition of high-frequency small amplitude and low-frequency large amplitude transverse oscillations $x(t) = \eta(t) + X(t)$ (see [3, 4] and references therein). For a standing wave formed by laser field the former is caused by the external high-frequency field force $\sim \cos(\omega t)$, and the effective potential is introduced to describe the latter. For a standing wave formed by two counter propagating P-polarized lasers the potential takes the following form [4, 5]

$$U_{\text{eff}}(x, \beta) = \frac{2\pi q^2 I}{\gamma m c \omega^2} \left(\beta_{\parallel}^2 - 1/2\right) [1 - \cos(2xk)], \tag{1.1}$$

where γ, $\beta_{\parallel}$, q and m are the particle Lorentz-factor, the longitudinal speed, the charge and mass, I and ω are the lasers intensity and frequency. The potential is of ponderomotive nature and due to its periodic structure is often addressed as an Optical Lattice (OL). If the particle transverse motion energy is less that the potential height, it becomes trapped in channeling regime and moving along an OL channel performs transverse oscillations within it [4–8].

Usually to describe various aspects of this motion and accompanying radiation an infinite channel length case is considered. However, the processes of particles injection and ejection in an OL, which is typically limited in space, could be of particular interest for future experiments and research on new methods for charged particle beams steering, shaping and diagnostics. That is why in this report we focus on ejection of relativistic ($\sim$ MeV) trapped charged particles from finite optical lattice formed by two counter-propagating P-polarized laser beams. In particular, we analyze the ejection angle θ at which a particle leaves OL. Radiation losses at the parameters considered here are less than 1 eV per cm (see in [9]), which is negligible comparing to total particle energy of several MeV, and hence are omitted.

2 Particle ejection from optical lattice

Let the optical lattice be formed by two identical counter propagating P-polarized laser beams with frequency ω and maximum total intensity I_m. Both lasers are parallel to the transverse Ox-axis. The lattice potential wells as well as the intensity profile along longitudinal z-axis are shown on the left plot of figure 1. Particle dynamics in the region of uniform intensity has a thorough classical description that could be found elsewhere [4, 8, 10, 11]. Below we consider electron dynamics in the region where the OL field declines. We call it ejection region of OL.
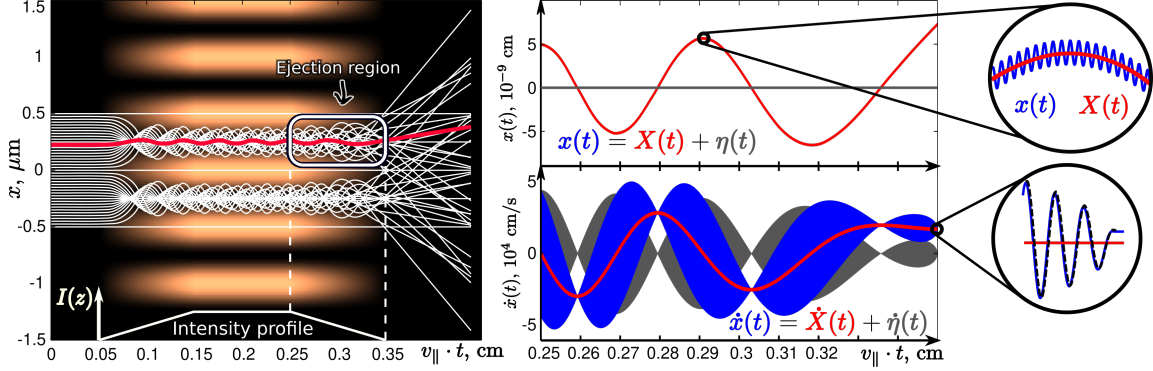
Figure 1. Left: general scheme of the considered system with highlight of the considered ejection region. Right (top): numerically simulated and analytically derived averaged (red) and total (blue) transverse oscillations; right (bottom): averaged (red), high-frequency (gray) and total (blue) transverse speed oscillations for 1.87 MeV electron in 1 mm wide ejection region of OL, formed by two intense $I = 1.2 \cdot 10^{14}$ W/cm^2 lasers of $\lambda = 1\,\mu$m wavelength. The red curve represents trajectory of the same electron (left and right).

2.1 Averaged oscillations in ejection region

Transverse intensity profile of a laser beam usually considered to be Gaussian. For the considered system the profile is represented with a function $I(z)$ and is chosen to be linear for the following reasons: (i) to simplify the form of the effective potential so that purely analytical solution could be presented, (ii) due to the fact that such a channeled particle could effectively feel such a linear intensity profile in a system when the laser intensity linearly declines with time, so that the decline of laser field with time could be transformed (by analogy with [12]) into intensity decline for the particle in longitudinal direction $I(z) \equiv I(v_\parallel t)$. Hence, for the OL exit ramp total field intensity is $I(z) = I_m(d - z)/d$ and the ejection region effective averaged potential is defined by the expression

$$U(x, z) = U_m \frac{d - z}{d} \left(1 - \cos\left(2kx\right)\right) \tag{2.1}$$

For the case of relativistic charged particle we consider z-component of its velocity (longitudinal speed) $v_\parallel$ to be constant if $U_m \ll \sqrt{p_\parallel^2 c^2 + m^2 c^4}$. Therefore, neglecting the longitudinal component of ponderomotive force, the effective averaged force inducing particle channeling oscillations can be reduced by the operator $\bar{\mathbf{F}} \equiv -\nabla U(x, z) \approx -\hat{\mathbf{e}}_x \partial U(x, z)/\partial x$. The equation of motion describing channeling oscillations near channel bottom

$$\gamma m \ddot{X}(t) = \kappa(at - 1)X(t), \tag{2.2}$$

with the following denominations $\kappa = 4k^2 U_m/d$ and $a = 1/t_e$. In case of particle initial excursion in ejection region $X(0) = X_0$ and transverse speed $\dot{X}(0) = V_0$ the solution of eq. (2.2) is

$$X(t) = \frac{\pi}{\gamma m a \kappa} \left\{ \text{Bi}\left(\frac{\kappa(at-1)}{(a\kappa)^{2/3}}\right) \left((a\kappa)^{2/3} V_0 \text{Ai}\left(-\frac{\kappa}{(a\kappa)^{2/3}}\right) - a\kappa X_0 \text{Ai}'\left(-\frac{\kappa}{(a\kappa)^{2/3}}\right) \right) \right.$$
$$\left. + \text{Ai}\left(\frac{\kappa(at-1)}{(a\kappa)^{2/3}}\right) \left(-(a\kappa)^{2/3} V_0 \text{Bi}\left(-\frac{\kappa}{(a\kappa)^{2/3}}\right) + a\kappa X_0 \text{Bi}'\left(-\frac{\kappa}{(a\kappa)^{2/3}}\right) \right) \right\}$$

(2.3)

This solution is applicable for ejection region of OL for the variable t changing from zero at the beginning of the ramp to t_e at its end — and for the Airy functions argument from $-\left|\kappa(a\kappa)^{-2/3}\right|$ to zero — which implies growth of averaged oscillations amplitude with time. On the contrary, the amplitude of averaged oscillations speed $\dot{X}(t)$ declines with time. Such behavior is illustrated on the plots of figure 1. On the right plot one can find comparison of the solution (2.3) for $X(t)$ and $\dot{X}(t)$ (red curves) with numerically simulated $x(t)$ and $\dot{x}(t)$ (blue curves).

Let us evaluate the ejection angle Θ of 3.46 MeV electron with initial $\dot{X}(0) = 0$ and $X(0) = 5 \cdot 10^{-9}$ cm as a function of ejection region length d. For $d \to 0$ ejection region is small and both X and $\dot{X}$ do not change significantly so that averaged transverse speed $\dot{X}(t_e)\big|_{d\to 0} \to V_0$. In case of longer ejection region the electron performs some fraction — or some number — of averaged oscillations and leaves OL with averaged transverse speed $\dot{X}(t_e)$. Noteworthy, the parameter d may be adjusted so that averaged transverse speed at the end of ejection region is maximal (figure 2, $d = d_m$), which could be particularly interesting for particles deflection using OL.
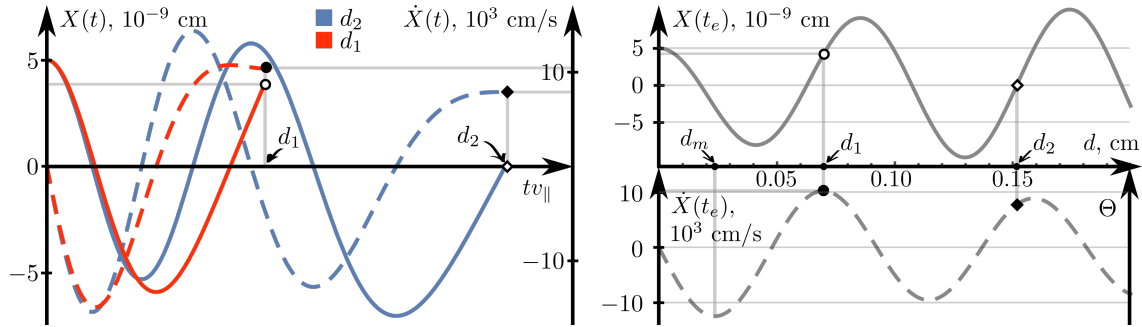
Figure 2. Left: 3.46 MeV electron averaged transverse excursion and speed within ejection region for two values of d ($d = d_1$ and $d = d_2$) and corresponding ejection angle Θ; right: transverse averaged excursion X and speed $\dot{X}$ at the end of ejection region $z = d$ as a function of parameter d.

Together with the averaged oscillations channeled particle performs Rapid Oscillations (RO) with frequency of the laser field. But the expression (2.3) de facto defines the particle trajectory since the rapid transverse oscillations amplitude is by definition much less than of the averaged one. However, this relation is not necessarily true for amplitudes of rapid and averaged speed oscillations. Is the angle defined solely by $\dot{X}(t_e)$? Or does rapid oscillations influence ejection direction too? To address these questions below we examine the speed of rapid oscillations.

2.2 Rapid transverse speed

Numerically calculated both trajectory and velocity of rapid oscillations are outlined in figure 1. One may notice that $\dot{\eta}$ (gray) and $\dot{X}$ (red) amplitudes are comparable inside ejection region.

The rapid oscillations are caused by high-frequency Lorentz force. In the case of P-polarized lasers the force electrical component is parallel to the longitudinal horizontal Oz-axis, while the magnetic component of Lorentz force has a dominating transverse Ox term, since $p_\parallel \gg p_x$ and $\mathbf{H}(t, x, z) = \hat{\mathbf{e}}_y H_y(t, x, z)$. Therefore, the equation of motion for the rapid oscillations is

$$\ddot{\eta}(t) = \frac{q\beta_\parallel}{\gamma m} H_y = \frac{q\beta_\parallel}{\gamma m} 2 H_m \sin{(X(t)k)} \sqrt{\frac{d - v_\parallel t}{d}} \cos(\omega t), \tag{2.4}$$

after its integration, we get the following solution

$$\dot{\eta}(t) = \mathcal{K} \int X(t) \sqrt{1 - at} \cos(\omega t)\, dt \tag{2.5}$$

While successful integration may be arduous, it is possible to estimate the integral in two major cases.

On one hand, for d of the same order as the laser wavelength λ, $d \sim \lambda$, only a few full rapid oscillations take place within ejection region. Moreover, as previously underlined, the amplitude of rapid oscillations $\eta(t)$ is very small (top right plot in figure 1), i.e. the value $X(t)$ changes insignificantly, so eq. (2.5) can be presented as follows

$$\dot{\eta}(t)\Big|_{d \sim \lambda} \approx \dot{\eta}_1(t) = \mathcal{K} \int_0^{t_e} \left(X(0) + t\dot{X}(0) + \frac{t^2}{2} \ddot{X}(0) \right) \sqrt{1 - at} \cos(\omega t)\, dt \tag{2.6}$$

In such a small ejection region the square root $\sqrt{1 - at}$ quickly goes from 1 to 0 on the scope of λ, therefore, the rapid oscillations become non-harmonic.

On the other hand, in case of $d \gg \lambda$ the ejection region span might be divided into two parts. Thus, for the first part $z < z_n$ ($z_n = v_\parallel NT$ where $T = 2\pi/w$ is the RO period and N is the number of RO periods T in t) the function $\mathcal{G}(t) = X(t)\sqrt{1 - at}$ changes slowly compared to $\cos(\omega t)$, and the motion still can be presented in the form of averaged trajectory $X(t)$ and harmonic oscillations $\eta(t)$. Therefore, the expression for integral solution (2.5) can be approximated by

$$\dot{\eta}(t)\Big|_{d - v_\parallel t \gg \lambda} \approx \dot{\eta}_2(t) = \mathcal{K} \left\{ \mathcal{G}(NT) \int_{NT}^{t} \cos(\omega\tau)\, d\tau + \sum_{n=0}^{N} \mathcal{G}(nT) \int_0^T \cos(\omega\tau)\, d\tau \right\} \tag{2.7}$$

Whereas for the rest of ejection region closer to the end of OL the square root changes considerably on the scale of a single rapid oscillation period, the rapid oscillations become non-harmonic and similarly to the case of $d \sim \lambda$ the speed of rapid oscillations for ($z > z_n$) can be evaluated by

$$\dot{\eta}(t)\Big|_{d - vt \sim \lambda} \approx \dot{\eta}_3(t) = \dot{\eta}_2(NT) + \\ + \mathcal{K} \int_{NT}^{t} \left(X(NT) + (\tau - NT)\dot{X}(NT) + \frac{(\tau - NT)^2}{2} \ddot{X}(NT) \right) \sqrt{1 - a\tau} \cos(\omega\tau)\, d\tau \tag{2.8}$$

Both expressions (2.7) and (2.8) imply the final rapid oscillations speed $\dot{\eta}(t_e)$ to be mainly defined by only several last periods in ejection region and allow analyzing the dependence of $\dot{\eta}(t_e)$ and, hence, $\dot{x}(t_e) = \dot{\eta}(t_e) + \dot{X}(t_e)$ from the ejection region width d presented in figure 3.
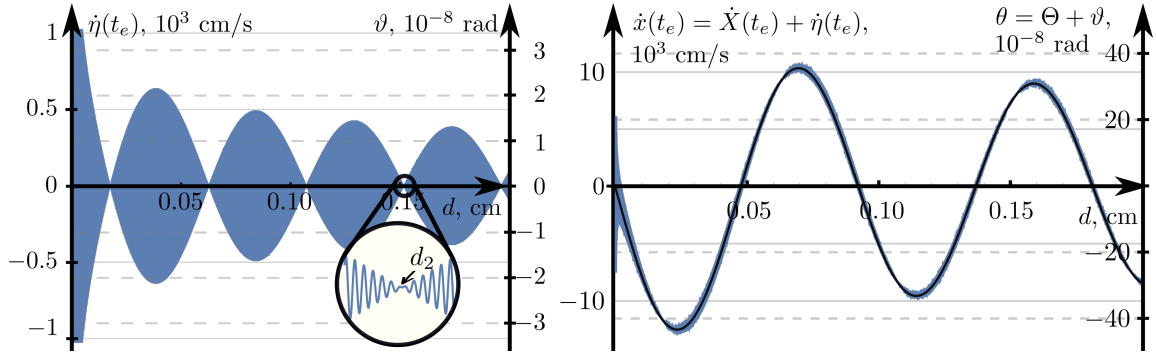
Figure 3. Left: 3.46 MeV electron RO ejection speed $\dot{\eta}(t_e)$, its contribution ϑ to total ejection angle; right: total transverse ejection speed $\dot{x}(t_e)$ and ejection angle θ as functions of ejection region width d.

The RO ejection speed $\dot{\eta}(t_e)$ is rapidly oscillating, and its amplitude is variable following the behavior of $X(t_e)$, so that e.g. $\dot{\eta}(t_e)$ for $d = d_1$ is close to zero. For small d possible values of $\dot{\eta}(t_e)$ described by (2.6) are very high defined by high intensity field of OL and could be comparable with $\dot{X}(t_e)$ (see right plot of the figure 3). Additionally, for larger values of d corresponding to $\dot{X}(t_e)$ close to zero, the total $\dot{x}(t_e)$ is solely defined by $\dot{\eta}(t_e)$. Finally, increasing d makes values of $\dot{\eta}(t_e)$ decrease together with the field intensity, at which the last rapid oscillations in ejection region take place.

3   Ejection angle

The analysis provided for transverse ejection speed $\dot{\eta}(t_e)$ and $\dot{x}(t_e)$ could be applied to the ejection angle θ, since the contribution for both averaged Θ and rapid speed oscillations ϑ to the electron ejection angle are $\theta \equiv p_\perp/p_\parallel \approx \left(\dot{X}(t_e) + \dot{\eta}(t_e) \right) / v_\parallel = \Theta + \vartheta$. Therefore, there is no need to repeat all the conclusions made for ejection speed as well as its components, and we supply all the figure with an appropriate ejection angle axis.

One important note concerning the angle values though becomes necessary. Both figures 2 and 3 are plotted for 3.46 MeV electron oscillating near a channel bottom of OL formed by two $I \sim 10^{14}$ W/cm² $\lambda = 1$ μm lasers. Lasers time envelope could have linear ramps so that intensity affecting channeled particle could be described by the plot at figure 1 (bottom left). The electron initial excursion $X_0 = 5 \cdot 10^{-9}$ cm is chosen small enough for parabolic potential approximation to be applicable and, hence, analytical description of averaged motion in such a parabolic potential possible. Increasing X_0 on one hand proportionally increases maximum values for ejection angles from indiscernible tens of nanoradians to tens of microradians for $X_0 \sim \lambda/4$ and 1.87 MeV electron, which could be useful for effective deflection of charged particles. On the other hand, large averaged oscillations amplitude implies the equation for averaged motion to be nonlinear, hence, approachable only by means of numerical analysis. The latter though in the light of the results above presented might be simplified to averaged motion description everywhere in the OL except the last several rapid oscillations, which need to be taken into account for appropriate ejection angle description. This could save much calculation time due to the fact that averaged oscillations frequency is considerably less than of the rapid ones.

4 Conclusion

The presented analysis of ejection speed and angle for a relativistic charged particle leaving OL proves rapid oscillations could introduce a significant contribution to those values, especially in the cases of short ejection region or small averaged ejection velocity $\dot{X}(t_e)$. The dynamics within ejection region is defined solely by averaged effective potential except for the several last high-frequency oscillations, where averaged speed and coordinate are almost constant, while $\dot{\eta}(t)$ can change the ejection angle considerably. This information is important for numerical simulations, since it makes possible to avoid time consuming calculations for rapid oscillations everywhere within OL except for the few last ones at the edge of ejection region. Indeed, the RO contribution is effectively defined by only a handful of the last non-harmonic oscillations in ejection region, while all other rapid oscillations according to the Kapitza method might be represented by harmonic oscillations of known variable amplitude. Even in case of different intensity profile (e.g. Gaussian) this conclusion is true, meaning that the whole trajectory could be evaluated with averaged potential except for several last high-frequency oscillations. This could considerably simplify numerical simulations for charged particles channeling in OL and accompanying radiation.

References

[1] P.L. Kapitza and P.A.M. Dirac, *The reflection of electrons from standing light waves*, *Math. Proc. Camb. Phil. Soc.* **29** (1933) 297.

[2] H. Batelaan, *The Kapitza-Dirac effect*, *Contemp. Phys.* **41** (2000) 369.

[3] A.V. Serov, *Ponderomotive nongradient force acting on a relativistic particle crossing an inhomogeneous electromagnetic wave*, *J. Exp. Theor. Phys.* **92** (2001) 20.

[4] S. Dabagov, A. Dik and E. Frolov, *Channeling of electrons in a crossed laser field*, *Phys. Rev. ST Accel. Beams* **18** (2015) 064002.

[5] E.N. Frolov, A.V. Dik and S.B. Dabagov, *Space charge effect simulation at electrons channeling in laser fields*, *Nucl. Instrum. Meth.* **B 402** (2017) 220.

[6] M.V. Fedorov, K.B. Oganesyan and A.M. Prokhorov, *Free-electron laser based on the effect of channeling in an intense standing light wave*, *Appl. Phys. Lett.* **53** (1988) 353.

[7] A.V. Andreev and S.A. Akhmanov, *Channeling, collimation, and radiation of relativistic electrons in ultrastrong nonuniform optical fields*, *J. Exp. Theor. Phys. Lett.* **53** (1991) 18 [http://www.jetpletters.ac.ru/ps/1146/article_17343.shtml].

[8] A.L. Pokrovsky and A.E. Kaplan, *Relativistic reversal of the ponderomotive force in a standing laser wave*, *Phys. Rev.* **A 72** (2005) 043401.

[9] A.V. Dik, S.B. Dabagov and E.N. Frolov, *Cooling of ultrarelativistic β and μ particles by laser channels*, *J. Phys. Conf. Ser.* **732** (2016) 012002.

[10] I.A. Andriyash, P. Balcou and V.T. Tikhonchuk, *Collective properties of a relativistic electron beam injected into a high intensity optical lattice*, *Eur. Phys. J.* **D 65** (2011) 533.

[11] P.W. Smorenburg, J.H.M. Kanters, A. Lassise, G.J.H. Brussaard, L.P.J. Kamp and O.J. Luiten, *Polarization-dependent ponderomotive gradient force in a standing wave*, *Phys. Rev.* **A 83** (2011) 063810.

[12] M.A. Efremov and M.V. Fedorov, *Classical and quantum versions of the Kapitza-Dirac effect*, *J. Exp. Theor. Phys.* **89** (1999) 460.